J Wood Sci (2004) 50:307–314
DOI 10.1007/s10086-003-0566-2

ORIGINAL ARTICLE

Jonas Blomberg · Bengt Persson

Plastic deformation in small clear pieces of Scots pine (*Pinus sylvestris*) during densification with the CaLignum process

Received: March 12, 2003 / Accepted: June 30, 2003

Abstract Specimens made of clear wood from Scots pine (*Pinus sylvestris* L.) were compressed semi-isostatically at 25°C in a Quintus press. Pressure ranged from 0 to 140 MPa and the maximum decrease in the crosscut area was about 60%. Quarter-sawn and plain-sawn specimens were densified with the inside face (pith side) up or down. A laser-made dot grid on the crosscut area of the uncompressed specimen was used to calculate plastic strains by image analysis of the displacement of dots after compression. Multivariate models were developed to determine the causes of deformation. The lower face was restrained by the press table and remained flat whereas sides attached to the rubber diaphragm became more irregularly shaped when compressed. Most of the total compression occurred below 50 MPa and was determined exclusively by pressure. Above 50 MPa, wood density was more important and compression was lower in the interior of specimens and in heartwood. Plastic compressive strain occurred predominately in the radial direction and toward the rigid press table. Strains were dependent on the sawing pattern and orientation. The growth rings of quarter-sawn specimens oriented with the outer face (bark side) down tended to buckle.

Key words Compressed wood · Plastic strain · Quintus press · Multivariate models

Introduction

In order to improve the hardness and other mechanical properties of wood there has long been a drive to develop processes for the densification of wood.[1] To date, the products have not been widely used, owing to high costs, capacity, and technical problems with the products.

CaLignum is the novel and patented process for wood densification through semi-isostatic compression in a Quintus press (Flow Pressure Systems, Sweden). CaLignum is also the name of the product. The Quintus press can yield pressures of up to 140 MPa, mediated through a flexible oil-filled rubber diaphragm that is pressed against a rigid press table or tool half. The press was originally developed for flexforming[2,3] of sheet metal for prototype and short series production. The CaLignum process makes it possible to densify wood of board size on an industrial scale.

In the process, the rubber diaphragm surrounds the wood pieces tightly, except against the steel table. As pressure increases, the weakest structures collapse in their weakest direction. Harder structures are not crushed or dislocated, and can protrude. Consequently, the densified wood may have an uneven shape.

The relationships between forces applied to wood and deformations are well known.[4–6] Gibson and Ashby[7] divided the deformation of wood in compression into three stages. In radial and tangential compression at small strains (<0.02), the deformation is linear–elastic, associated with cell wall bending.[7] Further loading causes bending and collapse of the cell walls by plastic hinges[8] and rapid deformation. Once the weak parts of the wood structure have collapsed, further stress causes minor, predominately elastic strain that will spring back immediately. Because wood is a viscoelastic and rheological material, the degree of deformation depends on the duration of load and part of the spring back is delayed.[9]

The stress–strain curves are similar in the radial and tangential directions, whereas collapse in axial deformation demands up to ten times higher stress. Tabarsa and Chui[10] state that in radial compression the last consolidation stage is dominated by elastic deformation of latewood, and in the tangential direction the last stage begins after readjustment of latewood layers by buckling. Radial compression causes nonuniform deformation starting in the weakest structures, the first-formed earlywood, and then propagating across the

J. Blomberg
Department of Wood Technology, Luleå University of Technology, Skellefteå Campus, SE-931 87 Skellefteå, Sweden

J. Blomberg (✉) · B. Persson
Department of Mathematics, Natural Science and Technology, Dalarna University, SE-781 88 Borlänge, Sweden
Tel. +46 23 77 86 67; Fax +46 23 77 86 01
e-mail: jbl@du.se

growth ring.[7,11,12] Rays buckle or collapse, which makes the deformation more plastic in the radial direction than in the tangential direction.[13,14] The tendency of ray buckling increases when the surrounding wood is weak. Thus, earlywood density is the most important factor controlling strength in the radial direction.[10] However, in softwoods with low wood density, like western red cedar (*Thuja plicata* D. Don.), stress at the proportional limit is found to be slightly higher in the radial direction than in the tangential direction[11,15] and much higher than when loaded statically with a ring angle of 45°.[15–17] Thus, rays work as reinforcements.[18] For softwoods with high wood density like Douglas fir (*Pseudotsuga menziesii* (Mirb.) Franco), stress at the proportional limit is found to be much higher in the tangential direction than in the radial direction. For both species, the modulus of elasticity is lowest in the tangential direction.[11,15] Tangential stress causes uniform cell collapse. In softwood, latewood bands form stiff reinforcement and the amount of latewood is the controlling factor for compressive strength in the tangential direction.[16] The plastic deformation of the cell walls corresponds to the buckling of the growth rings.

There are only a few studies of the isostatic compression of wood. Under isostatic conditions, wood will collapse in its weakest direction and when collapsed it will be further densified homogenously. Because axial compressive strength is substantially higher than the transverse compressive strength, axial compression will be negligible. Arakawa et al.[19] compressed sugi (*Cryptomeria japonica* D. Don) heartwood with water, after having sealed the surface with silicone to prevent water uptake. The wood was compressed to 60% of its original volume. They found that most deformation was in the earlywood and in the radial direction. Because the pressure was only 2 MPa, heating was needed for densification. Trenard[20] tested small pieces of several woods that were sealed with a thin rubber membrane and pressed in a hydraulic water-filled cylinder with up to 200 MPa pressure. Sapwood of Scots pine (*Pinus sylvestris* L.) was less densified than heartwood. The stress–strain curve found by Trenard can be divided into three parts: (1) only small strains (5%) occurs up to 5 MPa, (2) strain develops from 5% at 5 MPa to about 45% at 50 MPa, and (3) between 50 and 200 MPa, only 5% additional strain occurs. There was delamination in the middle lamella in earlywood and between rays and neighboring tracheids. It is likely that the deformation is different in the CaLignum process because the pressure is not hydrostatic. The result is probably influenced by how the piece is oriented relative to the steel table.

The objectives of this study were to determine how compression develops during the CaLignum process, how densification varies within a specimen, and what controls the shape of the densified specimen. In order to optimize the process, models are developed to describe what determines the compression and deformation.

Materials and methods

Clear specimens without defects, of length 100 mm, width 100 mm, and thickness 50 mm, were sawn from butt logs of Scots pine (*Pinus sylvestris* L.) with top diameter above 280 mm. The specimens were very homogenous with high basic density and low and even annual ring width. The specimens were plain-sawn or quarter-sawn and compressed with the outside (bark side) or inside (pith side) face against the press table (Fig. 1). The wood was at room temperature and no additional heat was added in the process. The moisture content ranged between 8% and 10%.

A 5 × 5-mm grid was burnt on the crosscut surface with a CO_2 laser (power: 100 W, opening-time: 0.15 s, focal distance: 15 mm) positioned by a robot.

The air-dry density (ρ_{origin}) of specimens (u = 8%–10%) was determined with an accuracy of 1.8 kg/m^3 by callipering (accuracy of calliper = 0.03 mm, repeatability = 0.01 mm) and weighing with a balance (Mettler Toledo BA4100S, readability = 0.01 g, repeatability = 0.008 g). The position of the pith and the distance from the pith to the heartwood border were determined using a transparent plastic film with concentric semicircles that was superimposed on the crosscut of the specimens to fit the curvature of the growth rings.

Specimens oriented as **A** and **B** in Fig. 1 were compressed at 10 pressure levels: 3, 5, 7.5, 10, 15, 20, 30, 50, 90, and 140 MPa were used for statistical analysis. There were

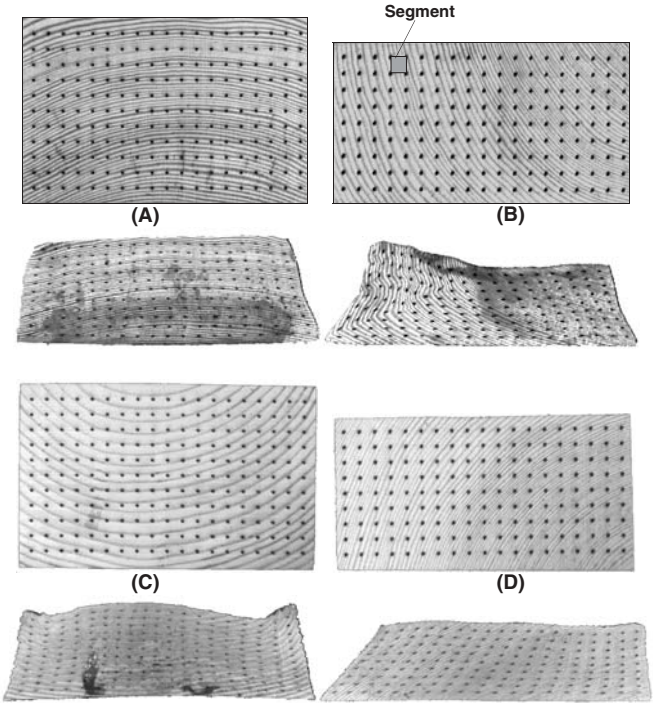

Fig. 1. Plain-sawn (**A**, **C**) and quarter-sawn (**B**, **D**) specimens prior to and after densification at 140 MPa. Dot grids (5 × 5 mm) burned with a laser divide the specimens into 180 segments in the plain-sawn specimens and 144 segments in the quarter-sawn specimens. Specimen **A** and **D** are compressed with the inside face against the press table, **B** and **C** are compressed in the opposite orientation

Table 1. Characteristics of plain-sawn and quarter-sawn specimens

Variable	Plain-sawn	Quarter-sawn
Wood density, ρ_{origin} (kg/m^3)	535 (71)	533 (50)
Least distance from specimen to pith (mm)	7.75 (2.20)	3.74 (1.54)
Heartwood percentage	50.3 (25.2)	33.8 (14.6)
Mean annual ring width (mm)	2.1 (1.0)	1.5 (0.4)
Latewood content (%)	26.7 (5.6)	26.9 (18.4)

Values given are means with standard deviations in parentheses

one or two plain-sawn and quarter-sawn specimens per pressure level in the interval 3–90 MPa and three and four specimens, respectively, compressed to 140 MPa. Four of each type of specimen oriented as **C** and **D** in Fig. 1 were also compressed at 140 MPa. Characteristics of plain-sawn and quarter-sawn specimens are given in Table 1.

Images of the laser-gridded surfaces were captured with a Sony XC003P CCD colour camera (570 × 756 pixels) before and after compression. Using image analysis with Scion Image (Release Beta 3B, 1998, Scion Corporation, Frederick, MD, USA) the grid dots were eroded to one pixel each, the coordinates of which were used for measurements of deformations and strains. The tetragon between four dots defined a segment. Plain-sawn specimens had 180 such segments and quarter-sawn specimens had 144.

A greyscale value for the transition between earlywood and latewood, according to Mork,[21] were determined visually and used for thresholding images taken before compression. Ring width and latewood content were then measured along radial-oriented lines.

The analysis focused on three response variables: (1) degree of compression (ε_{area}), (2) remaining maximum extent after compression in radial relative to tangential direction (R/T), and (3) remaining maximum extent parallel to the press table relative to the perpendicular direction (X_{max}/Y_{max}). The variables were calculated for each segment and in all cases the plastic strains were assessed after relaxation of pressure. ε_{area} was defined as $1 - (A_c/A_0)$, where A_0 and A_c are the area of a crosscut surface before and after compression, respectively. ε_{area} is close to the volume strain because strain in the axial direction is negligible. R/T was defined as $(1 - \varepsilon_{rad})/(1 - \varepsilon_{tang})$, where the radial and tangential compressive strains (ε_{rad} and ε_{tang}) were estimated for each segment with regression analysis using the model:

$$L_i^2 = \varepsilon_{rad}^2 \cdot r_i^2 + \varepsilon_{tang}^2 \cdot t_i^2 + \in_i$$

where L represents the six distances between the dots in a segment after compression (see Fig. 2), and the coefficients r_i and t_i are the distances in the radial and tangential directions between the dots before compression which are estimated trigonometrically from the distances between dots and the angle of the annual rings at the midpoint between dots. $\in_i$ is the random error. A high R/T means that the compressive strain is high in the tangential direction relative to the radial direction. A high value of X_{max}/Y_{max} occurs when the segment is elongated horizontally.

In the analyses, the specimens were characterized by pressure (σ_{Press}) and wood density (ρ_{origin}). The positions of

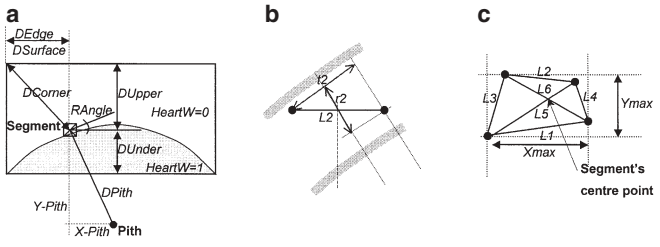

Fig. 2a–c. Description of the variables for characterizing specimens and segments. **a** Specimen before compression; **b** distance between two dots before compression; and **c** segment in compressed specimen

the segments were characterized by the distance to the midpoint from the pith (DPith), their components parallel and perpendicular to the press table (X-pith and Y-pith), as well as the shortest distance to the press table (DUnder), the upper side (DUpper), the nearest edge side (DEdge), nearest upper or edge side (DSurface), and the nearest upper corner (DCorner) (Fig. 2). From X-pith and Y-pith, the angle of growth rings (RAngle) was calculated. Ring width (RWidth) and latewood contents (LateW) were determined from DPith and the measurements of the growth ring and latewood widths. Latewood contents are the latewood proportion of the growth ring width. Finally, a dummy variable was used to characterize whether the segment predominately consisted of heartwood (HeartW = 1) or sapwood (HeartW = 0).

The variation in R/T, X_{max}/Y_{max}, and ε_{area} was analyzed using partial least squares (PLS) regression[22,23] in the software package SIMCA-P version 8.0 (Umetrics AB, Umeå, Sweden). Models were made for the whole material as well as for separate pressure levels (0–50 MPa and 50–140 MPa) and type of specimen (quarter-sawn and plain-sawn). Regressor variables that did not contribute substantially to the degrees of determination (R^2X, a measure of how well the variance in regressor variables is explained by the model, and Q^2, the predictive ability for new observations) were discarded in order to simplify the functions as much as possible. Residual analysis was performed by locating deviating observations (outliers) in the specimens.[24]

The development of the plastic compressive strains (ε_P) in segments with increased pressure (σ_{Press}) in the interval 0–140 MPa was analyzed using nonlinear regression analysis (PROC NLIN, method DUD in SAS statistical package, release 8.02, SAS Institute, Cary, NC, USA). Separate analyses were made for ε_{area}, ε_{rad} and ε_{tang}. The following model was used:

$$\varepsilon_P = b_0 \cdot \left(1 - e^{-b_1 \cdot \sigma_{Press}}\right) + \epsilon_i \quad (1)$$

Results

The relationships between pressure and plastic compressive strain is shown in Fig. 3. Separate stress–strain curves according to Eq. 1 are shown for plain-sawn specimens oriented with the inside face down and for quarter-sawn specimens with the outside face down (see types **A** and **B** Fig. 1). There was no significant difference in the development of plastic area strain of the crosscut area (ε_{area}) between the plain-sawn and quarter-sawn specimens. Strain increased steadily with increased pressure to about 50 MPa, after which further plastic compression was limited. Strain asymptotically approached a level of almost 50% (b_0 according to Eq. 1).

Development of radial compressive strain (ε_{rad}) differed between plain-sawn and quarter-sawn specimens. Plain-sawn specimens tended to collapse in the radial direction at lower pressure compared with the quarter-sawn ones, but the difference decreased at higher pressure. The segments of plain-sawn specimens with the inside face down were very evenly shaped after compression (**A** in Fig. 1) and the segments of quarter-sawn specimens with the outside face down were the most irregularly shaped (**B** in Fig. 1). The slope coefficient b_1 in Eq. 1 differed significantly but not the asymptote b_0. Tangential compressive strain (ε_{tang}) development was consequently, but not significantly, slower for quarter-sawn specimen than for plain-sawn ones. The asymptote was almost three times higher for radial strain than for tangential strain.

The coefficients and the degrees of determination from the PLS-regression functions of responses in individual segments are given in Tables 2, 3, and 4. There was no clear difference between plain-sawn and quarter-sawn specimens in the interval 0–50 MPa. The degrees of determination, Q^2, and R^2X were generally highest for the functions predicting the variation in ε_{area}; and pressure alone explained 85% of the variation whereas no other regressor variables contributed substantially (Table 2). Pressure was also the most important factor controlling X_{max}/Y_{max} (Table 4), whereas R/T was predominantly determined by original density (ρ_{origin}, Table 3) between 0 and 50 MPa.

In the consolidation phase in the interval 50–140 MPa, the functions were less determined by pressure, they had lower Q^2 and R^2X, and were more complicated. ρ_{origin} was the most important factor explaining ε_{area} (Table 2). The functions were quite similar for plain-sawn and quarter-sawn specimens as well as for the two types together. However, Q^2 and R^2X were lower when quarter-sawn specimens were involved.

In the pressure interval 50–140 MPa, it was difficult to find functions that could predict the variation in R/T and X_{max}/Y_{max} for plain-sawn and quarter-sawn specimens to-

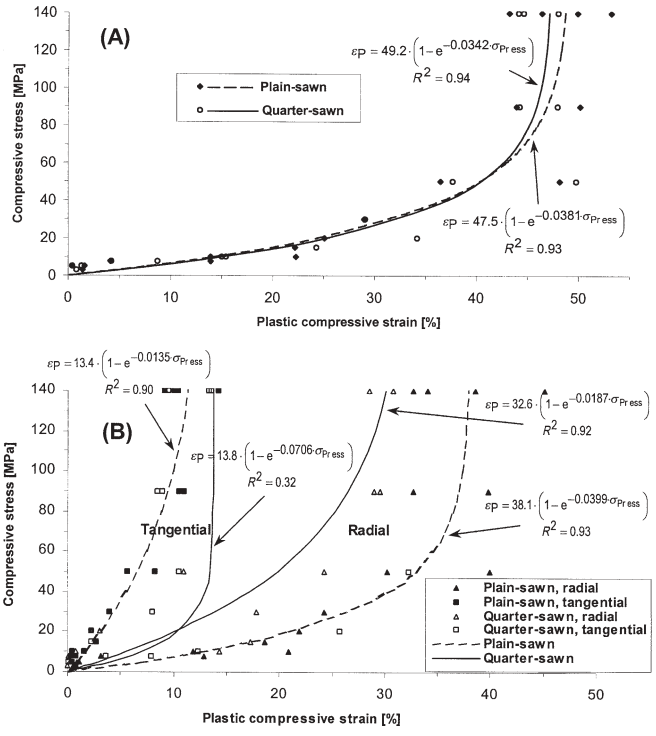

Fig. 3. Stress–strain curves for plastic compression in cross-cut area (**A**) and radial and tangential directions (**B**). Strains for plain-sawn and quarter-sawn specimen are separated. Each dot represents the average of one specimen. The functions were based on data for each segment

Table 2. Coefficients and degrees of determination of partial least squares (PLS) regression functions for the response variable ε_{area}

Type of specimen Pressure	Degrees of determination		Coefficients					
	Q^2	R^2X	Const	$\log_{10}[\sigma_{Press}]$	ρ_{origin}	DPith	HeartW	DUnder
All								
0–50	0.85	–	1.166	0.919				
50–140	0.59	0.57	7.720	0.276	**−0.586**	0.144	−0.185	0.059
Plain-sawn								
50–140	0.64	0.68	7.427	0.290	**−0.548**	0.100	−0.238	0.045
Quarter-sawn								
50–140	0.50	0.51	8.360	0.325	**−0.598**	0.200	−0.115	0.130

The independent variables contributing most to the degree of determination are written in bold numbers

Table 3. Coefficients and degrees of determination of PLS regression functions for the response variable *R/T*

Type of specimen Pressure	Degrees of determination		Coefficients							
	Q^2	R^2X	Const	$\log_{10}[\sigma_{Press}]$ (1)	ρ_{origin}	LateW	RAngle (4)	DPith	DEdge	1 × 4
All										
0–50	0.43	0.33	−0.390	−0.171	**−0.287**	−0.248	0.256			0.167
50–140	0.29	0.32	3.182	−0.181	−0.110	−0.185	**0.397**			
Plain-sawn										
50–140	0.51	0.56	4.570	0.022	0.228	−0.108	**1.050**	0.201	0.435	
Quarter-sawn										
50–140	0.37	0.37	2.930	−0.220	−0.227	−0.154	0.136	**0.236**		

The independent variables contributing most to the degree of determination are written in bold numbers

Table 4. Coefficients and degrees of determination of PLS regression functions for the response variable X_{max}/Y_{max}

Type of specimen Pressure	Degrees of determination		Coefficients							
	Q^2	R^2X	Const	$\log_{10}[\sigma_{Press}]$	ρ_{origin}	RAngle	D Pith	D Under	D Corner	D Surface
All										
0–50	0.56	0.69	3.605	**0.792**	−0.319			−0.309		
50–140	0.23	0.44	3.992		−0.142		−0.130	**−0.208**	0.139	0.132
Plain-sawn										
50–140	0.46	0.66	6.914		−0.339	0.323	−0.146	**−0.279**	0.088	−0.014
Quarter-sawn										
50–140	0.52	0.60	2.971		−0.310	**−0.388**	−0.235	−0.144	0.109	0.147

The independent variables contributing most to the degree of determination are written in bold numbers

gether; Q^2 became very low (Tables 3 and 4). For *R/T*, Q^2 was also low for the function for quarter-sawn specimens alone. Pressure and density influenced *R/T* differently for the two types of specimens, whereas ring angle (RAngle) and increasing distance from the rubber diaphragm (DSurface) influenced X_{max}/Y_{max} differently in plain-sawn and quarter-sawn specimens.

Ring angle (RAngle) was the most important regressor variable for predicting the variation in *R/T* of all specimens pressed to 50–140 MPa and of plain-sawn specimens alone (Table 3). This variation is visualized in Fig. 4. With higher ring angle, *R/T* increased, i.e., there was more tangential and less radial plastic compressive strain. At a given ring angle, *R/T* was higher for plain-sawn specimens than for quarter-sawn specimens. For annual ring angles of 55°–70°, there was a peak in *R/T* in quarter-sawn specimens as an effect of buckling of the annual rings (see **B** Fig. 1). In specimens with high ring angles, the peak *R/T* appears at higher angles. In the quarter-sawn specimen with ρ_{origin} below 450 kg/m^3 (solid line in Fig. 4), *R/T* was exceptionally high.

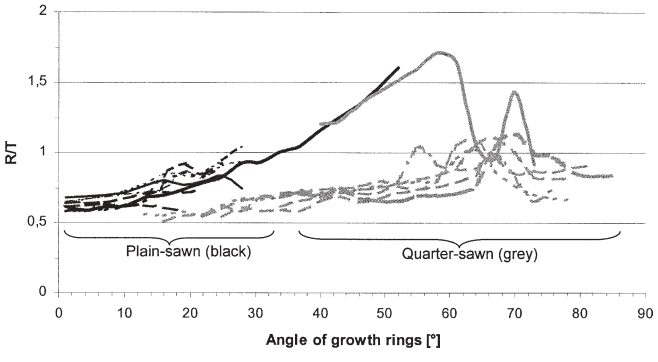

Fig. 4. The extent of segments in radial relative to tangential direction (*R/T*) as effect of the angle of annual rings. Each line represents one specimen pressed to 50–140 MPa. The lines are smoothed between the mean values at an interval of 3°. Specimens with air-dry density below 450 kg/m^3 are shown as *solid lines*

Discussion

The compression process

In terms of ε_{area}, the compression with the CaLignum process was reasonably homogenous and resulted in no dramatic checking or other disturbances. In part, this was an effect of testing only specimens without knots and other defects. The results may also be specific for the dimension tested. There have been earlier reports that the strength properties in transverse compression varies with the thickness and crosscut area of the specimen.[4,11,14]

Up to about 50 MPa, the plastic compressive strain of specimens increased with pressure, after which the stress–strain curve raised sharply and further plastic strain was small (Fig. 3). This resembles the common stress–strain curve for static compression,[7,10] but differs in that it expresses semi-isostatic compression and the plastic component only. The main differences were that the pressure level increased progressively with increased strain during the col-

lapse phase and that the steep rise of pressure occurred at a very high pressure of 50 MPa. This can be compared with the common stress–strain curve in which case the rise starts at or below the static compression strength of Scots pine wood perpendicular to grain, about 7.5 MPa.[25] Our findings coincide well with the compression curve of isostatic compression of Scots pine reported by Trenard.[20] Isostatic compression mediated with a rubber diaphragm or water is very flexible and the collapse will thus be less dramatic than at static compression between rigid loading plates, which can explain the slope of the stress–strain curve. After the pressure level started to rise steeply, most deformation is elastic, but latewood still collapses plastically to some extent.

The two parameters of greatest importance for the compression of wood are pressure and original wood density. Up to 50 MPa, ε_{area} was strongly determined by pressure (Table 2). Increased pressure also had a dominant importance for increasing X_{max}/Y_{max} (Table 4), which shows that the pressure was predominately static in the direction perpendicular to the press table. The compression was also predominately in the radial direction (*R/T* below 1; Figs. 3B, 4), as stated by e.g., Kennedy.[16] This tendency was more pronounced at higher pressure (Table 3). However, wood density was more important for *R/T*; wood with low density was prone to be compressed tangentially (Fig. 4), in accordance with Bodig.[15] Wood with low density was also prone to static strain perpendicular to the press table (X_{max}/Y_{max} decreased with ρ_{origin}; Table 4). It collapsed at low pressure, when pressure was almost completely static.

Above 50 MPa, in the phase when the cell wall densifies, compression was more complicated. Most compression had occurred at lower pressure, which made pressure of minor importance (Fig. 3). ε_{area} varied predominately with wood density (Table 2). The negative relationship between density and the degree of compression is well documented.[4–6,25] Heartwood also had a negative influence on ε_{area}, probably as an effect of high degree of elastic springback.[20] For X_{max}/Y_{max} and *R/T*, plain-sawn and quarter-sawn specimens responded quite differently. Generally, the specimens were flattened against the press table (increased X_{max}/Y_{max}) and they were predominately deformed in the radial direction (decreased *R/T*).

Radial strain was not observed to cause the collapse of rays in their axial direction; they were buckled and the angle between rays and growth rings was displaced. This displacement within the annual ring may be linked to the sometimes rhombic shape of the segments (Fig. 1).

Effects of sawing pattern and orientation of specimens

Plain-sawn and quarter-sawn specimens had similar degrees of compression (ε_{area}; Fig. 3A; Table 2) and both types were predominately compressed in the radial direction (Figs. 3B, 4). In other respects, plain-sawn and quarter-sawn specimens performed very differently. The deformation also depended on the orientation of the specimens (inside or outside face down; Fig. 1). Most deformation was directed perpendicular to the press table and the specimens tended to become trapezoidally shaped with the largest side toward the press table (Fig. 1). In quarter-sawn specimens where growth rings had very steep angles, they tended to buckle (see **B** in Fig. 1). This variation between different types of specimens would not have occurred if the compression had been perfectly isostatic.

There are probably three factors behind the deviations from isostatic compression. First, the specimens were constrained on one side by the rigid press table, which makes one side remain flat, whereas the other sides can be formed more flexibly depending on the density and structure of the wood. Second, there is also a high coefficient of friction between wood and steel (μ = 0.2–0.5), which prevented compression of the lower face parallel to the press table. Finally, the pressure was static before the rubber diaphragm had fully embedded the specimens. Because the compression strength of Scots pine wood perpendicular to grain is only ca 7.5 MPa,[25] it is likely that the pressure was more static than isostatic when the structure started to collapse.

The trapezoid shape, which occurs in all kinds of specimens (Fig. 1), indicates that the rubber diaphragm started to fill the gaps between specimens before they collapsed. The width of the upper face decreased substantially, a clear indication that it was compressed perpendicular to the edges (Fig. 1). Where the midline between the edge and upper face was predominately in the radial direction the upper corners became rounded or obtusely angled, whereas when this midline was more tangentially directed the angle of the corner became acute (Fig. 1). The lower face did not decrease substantially in width. When the rubber diaphragm had penetrated down to the press table the specimens had probably already collapsed. In plain-sawn specimens, the lower face often became slightly wider, which may be an effect of straightening the annual rings as the wood collapsed radially.

Buckling of annual rings only occurred in quarter-sawn specimens oriented with the outside face down (see **B** in Fig. 1). Tendencies of buckling could be seen in quarter-sawn specimens pressed to 10 MPa, and more clearly in the specimen pressed to 20 MPa. Ring buckling typically occurs when softwood is compressed statically in the tangential direction.[10,15] The steepest growth rings were also those that were subjected to buckling, but not where ring angle was steepest (Fig. 4). The major buckles arose in the break point between the parts of the specimens having the lowest ring angle that collapsed radially and the parts with steep ring angle that are strained both radially from the edge and tangentially from above. Buckling often resulted in folds in radially oriented lines toward the outside corner (**B** in Fig. 1), sometimes combined with checking. Buckling altered the ring orientation so that further compression became more radial.

The growth rings of quarter-sawn specimens oriented with the inside face down never buckled (see **D** in Fig. 1). When the parts with low ring angle collapsed radially, the steeper growth rings became displaced and attained a much lower angle. In plain-sawn specimens oriented with the outside face down (**C** in Fig. 1), the growth rings with the

steepest angle were curved, but the ring angle was not steep enough for buckles to appear.

Variation within specimens

ε_{area} did not vary much within the specimens. However, when pressed with 50–140 MPa, ε_{area} was lowest close to the press table (low DUnder) and it tended to increase with distance from the pith (DPith; Table 2). DPith itself was not important, but describes the variation between plain-sawn and quarter-sawn specimens oriented as in **A** and **B** of Fig. 1. In plain-sawn specimens the highest DPith was at the outside face and particularly the corners, which were oriented upward. In quarter-sawn specimens the DPith was high at the edge with high ring angle and the corner where most buckling occurred. In both cases these were also the parts where the segments were most strained tangentially (high *R/T*; Table 3). Where DPith was high and DUnder low, X_{max}/Y_{max} was also high (Table 4), i.e., the segments were not flattened much toward the press table.

Analysis of the residuals from the PLS-regression functions for plain-sawn specimens pressed to 50–140 MPa showed that the models underestimate ε_{area} for segments close to the upper and lower surfaces. In the middle of the specimen, the models tend to overestimate ε_{area}. In quarter-sawn specimens, segments with underestimated ε_{area} were detected close to the upper corner closest to the pith. In the other three corners, models overestimated ε_{area}.

X_{max}/Y_{max} varied greatly between segments within the specimens, and also between plain-sawn and quarter-sawn specimens (Table 4). In plain-sawn specimens, X_{max}/Y_{max} was particularly high at the lower corners and low at the upper corners (**A** in Fig. 1). This is linked to the trapezoid shape of the specimens. In quarter-sawn specimens, X_{max}/Y_{max} is thus high close to the press table, but also high in the edge where ring angle was low. From this it is obvious that it is difficult to find a common function that explains X_{max}/Y_{max} well for both plain-sawn and quarter-sawn specimens pressed within the interval 50–140 MPa. The degrees of determination (R^2X and Q^2) for the presented function were also low (Table 4).

For *R/T* the common function for both plain-sawn and quarter-sawn specimens pressed within the interval 50–140 MPa also yielded poor R^2X and Q^2. The reason was that pressure and wood density had quite opposite effects on plain-sawn specimens compared with quarter-sawn specimens as well as all specimens in the pressure interval 0–50 MPa (Table 3). Once the rubber diaphragm filled the gaps between the test pieces, plain-sawn specimens tended to be pressed more tangentially, unless the shape became very trapezoidal. Quarter-sawn specimens were pressed radially, which resulted in more severe buckles. Within the specimens, individual segments were still relatively more strained tangentially where density or latewood contents were low. Latewood contents was registered on individual segments and acted in the function for plain-sawn specimens as a suppressor variable that modified the effect of globally assessed density.

Conclusions and practical implications

Using the CaLignum process, the specimens were compressed without major checks and other disturbances except buckling of growth rings and irregular shaping. Ring buckling can be avoided if plain-sawn members are used and if they are placed with the inside face against the rigid press table. Such members are also the most regularly shaped.

The CaLignum process means isostatic compression, although the compression is not perfectly isostatic. Upon collapse, the pressure is almost static. If the degree of isostatic pressure could be controlled, the shaping would also be better controlled. Purely isostatic pressure would make the shape very irregular. It would be possible to get isostatic pressure at an earlier stage if the gaps between members were filled with rubber. Thereby it would probably be possible to avoid trapezoidal shaping of members. Lowering the friction between the wood and the press table may also result in less trapezoidal shaping.

References

1. Wingate-Hill R (1983) A review of processes which involve compressing wood perpendicular to the grain. Aust Forest Res 13:151–164
2. Johannisson TG (1994) High pressure forming of body parts using flexible tools. Sheet Metal Ind 71:20–22
3. Skötte A (1976) Quintus sheet-metal forming presses – a new means for metal forming with high pressures and single tools. Sheet Metal Ind 53:212, 215–216, 219–220
4. Kollman FFP, Côté WA (1984) Principles of wood science and technology, vol 1. Springer, Berlin Heidelberg New York, pp 335–359
5. Wangaard FF (1950) The mechanical properties of wood. Wiley, New York, pp 27–39, 152–159
6. Dinwoodie JM (2000) Timber: its nature and behavior, 2nd edn. Spon, London, pp 164–165
7. Gibson LJ, Ashby MF (1997) Cellular solids: structure and properties, 2nd edn. Cambridge University Press, Cambridge, UK, pp 394–405
8. Tabarsa T, Chui YH (2000) Stress–strain response of wood under radial compression. Part I. Test method and influences of cellular properties. Wood Fiber Sci 32:144–152
9. Wolcott MP, Kamke FA, Dillard DA (1994) Fundamental aspects of wood deformation pertaining to manufacture of wood-based composites. Wood Fiber Sci 26:496–511
10. Tabarsa T, Chui YH (2001) Characterizing microscopic behavior of wood under transverse compression. Part II. Effect of species and loading direction. Wood Fiber Sci 33:223–232
11. Bodig J (1966) Stress–strain relationship for wood in transverse compression. J Mater 1:645–666
12. Ando K, Onda H (1999) Mechanism for deformation of wood as a honeycomb structure I: effect of anatomy on the initial deformation process during radial compression. J Wood Sci 45:120–126
13. Kunesh RH (1961) The inelastic behaviour of wood: a new concept for improved panel forming processes. Forest Prod J 11:395–406
14. Kunesh RH (1968) Strength and elastic properties of wood in transverse compression. Forest Prod J 18:65–72
15. Bodig J (1965) The effect of anatomy on the initial stress–strain relationship in transverse compression. Forest Prod J 15:197–202
16. Kennedy RW (1968) Wood in transverse compression. Forest Prod J 18:36–40
17. Hofstrand AD (1974) Transverse compression of inland Douglas Fir. Station Paper, Forest, Wildlife and Range Experiment Station, University of Idaho, pp 2–16

18. Schniewind AP (1959) Transverse anisotropy of wood: a function of gross anatomic structure. Forest Prod J 9:350–359
19. Arakawa T, Funato M, Hoshino A (1998) Development of a novel treatment process and its applications. 29th Annual Meeting of the IRG, Maastricht, Netherlands, June14–19, IRG-WP-98–40111
20. Trenard Y (1977) Study of the isostatic compressibility of some timbers. Holzforschung 31:166–171
21. Mork E (1928) Die Qualität des Fichtenholzes unter besonderer Rücksichtnahme auf Schleif- und Papierholz. Papier-Fabrikant 26:741–747
22. Wold S (1978) Cross-validatory estimation of the number of components in factor and principal components models. Technometrics 20:397–405
23. Geladi P, Kowalski BR (1986) Partial least-squares regression: a tutorial. Anal Chim Acta 185:1–17
24. Danvind J (2002) PLS prediction as a tool for modeling wood poperties. Holz Roh Werkst 60:130–140
25. Tsoumis G (1991) Science and technology of wood: structure, properties, utilization. 1. Chapman and Hall, New York, pp 164–175

The publication of this article was made possible by an Emachu Research Fund. The authors are greatful for the fund.